

# Examination of the Effect of Triangular Plate on the Performances of Reverse Rotating Dual Savonius Wind Turbines

## **Authors:**

Burcin Deda Altan, Afsin Gungor

*Date Submitted:* 2023-02-21

*Keywords:* Renewable and Sustainable Energy, Wind, Savonius turbine, dual, performance

## **Abstract:**

In the present study, the performance of the Savonius wind turbine in designs with dual turbines rotating opposite to each other was examined. To improve the performance of the Savonius wind turbine in the dual turbine design, a triangular plate was placed in front of the turbines. The effects of the geometric parameters of this triangular plate which was placed on the turbine performance were studied. The numerical analyses performed were confirmed by the experimental data of a previous study in the literature. The performance values of Savonius wind turbines were analyzed by numerical analysis, the accuracy of which was proven by experimental data. ANSYS Fluent, a computational fluid dynamics (CFD) program, was used for the performance analysis. In the first stage, the maximum power coefficient ( $C_p$ ) of the conventional Savonius wind turbine was obtained around 0.17. With the optimum geometric parameter studies, the maximum power coefficient of the Savonius wind turbine in the triangular plate dual turbine design was determined to be around 0.22. Thus, it was found that the power coefficient obtained by a single Savonius wind turbine in a triangular plate dual turbine design was around 30% higher compared to the power coefficient of the conventional Savonius wind turbine.

*Record Type:* Published Article

*Submitted To:* LAPSE (Living Archive for Process Systems Engineering)

*Citation (overall record, always the latest version):*

LAPSE:2023.0805

*Citation (this specific file, latest version):*

LAPSE:2023.0805-1

*Citation (this specific file, this version):*

LAPSE:2023.0805-1v1

*DOI of Published Version:* <https://doi.org/10.3390/pr10112278>

*License:* Creative Commons Attribution 4.0 International (CC BY 4.0)

## Article

# Examination of the Effect of Triangular Plate on the Performances of Reverse Rotating Dual Savonius Wind Turbines

Burcin Deda Altan \*  and Afsin Gungor

Department of Mechanical Engineering, Faculty of Engineering, Akdeniz University, Antalya 07058, Turkey

\* Correspondence: bdeda@akdeniz.edu.tr

**Abstract:** In the present study, the performance of the Savonius wind turbine in designs with dual turbines rotating opposite to each other was examined. To improve the performance of the Savonius wind turbine in the dual turbine design, a triangular plate was placed in front of the turbines. The effects of the geometric parameters of this triangular plate which was placed on the turbine performance were studied. The numerical analyses performed were confirmed by the experimental data of a previous study in the literature. The performance values of Savonius wind turbines were analyzed by numerical analysis, the accuracy of which was proven by experimental data. ANSYS Fluent, a computational fluid dynamics (CFD) program, was used for the performance analysis. In the first stage, the maximum power coefficient ( $C_p$ ) of the conventional Savonius wind turbine was obtained around 0.17. With the optimum geometric parameter studies, the maximum power coefficient of the Savonius wind turbine in the triangular plate dual turbine design was determined to be around 0.22. Thus, it was found that the power coefficient obtained by a single Savonius wind turbine in a triangular plate dual turbine design was around 30% higher compared to the power coefficient of the conventional Savonius wind turbine.



**Citation:** Altan, B.D.; Gungor, A. Examination of the Effect of Triangular Plate on the Performances of Reverse Rotating Dual Savonius Wind Turbines. *Processes* **2022**, *10*, 2278. <https://doi.org/10.3390/pr10112278>

Academic Editor: Zhiwei Gao

Received: 30 September 2022

Accepted: 31 October 2022

Published: 3 November 2022

**Publisher's Note:** MDPI stays neutral with regard to jurisdictional claims in published maps and institutional affiliations.



**Copyright:** © 2022 by the authors. Licensee MDPI, Basel, Switzerland. This article is an open access article distributed under the terms and conditions of the Creative Commons Attribution (CC BY) license (<https://creativecommons.org/licenses/by/4.0/>).

**Keywords:** renewable energy; wind; Savonius turbine; dual; performance

## 1. Introduction

As a result of the increasing interest in clean and renewable energy sources in recent years, wind energy has become one of the most developed and used energy sources. In order to get the most out of wind energy, the main factor in obtaining energy is wind turbines. These turbines are generally divided into two as horizontal and vertical axis turbines according to their rotation axis. To date, many studies on these turbines have been conducted and are still being conducted [1–4]. One of the wind turbines that has been studied considerably from the past to the present is the Savonius wind turbine, which is a vertical axis turbine. Especially since the construction of these turbines is quite simple and the cost is low compared to other wind turbines, many studies have been carried out and continue to be carried out to increase the power performance of Savonius wind turbines in order to increase their use. Santhakumar et al. [5] experimentally described the behaviour of a vertical axis Savonius turbine in lane highways. Abdelaziz et al. [6] conducted a three-dimensional numerical analysis to enhance the performance of a conventional Savonius turbine by using auxiliary blades. Norouztabar et al. [7] carried out a numerical analysis on the model of the triple-blade vertical Savonius turbine equipped with additional blades. Lee et al. [8] numerically investigated the performance and shape characteristics of a helical Savonius wind turbine at various helical angles. Sharma et al. [9] examined the coefficients of the performance of a Savonius turbine by adding concentric multiple miniature blades using numerical simulation software. Al Absi et al. [10] numerically and experimentally investigated the performance efficiency of Savonius elliptical turbines by developing the parameters of the blade shape and overlap ratio. Manganhari et al. [11] investigated the

performance of the rotor house for the three bladed Savonius turbine. Irabu et al. [12] experimentally investigated the performances of the Savonius turbine with the guide-box tunnel. In order to improve the low performance levels of Savonius wind turbines, a curtain arrangement was designed outside the turbine [13,14]. Tartuferia et al. [15] improved the aerodynamic performance of the Savonius wind rotor with new rotor blade designs. Chang et al. [16] designed a new blade profile in the form of interior design using numerical methods. Zhou et al. [17] developed a simulation method for predicting the Savonius rotor's aerodynamic performance. Goodarzi et al. [18] compared the effectiveness of the different endplates used with numerical simulation for the Savonius wind turbine. Mereu et al. [19] investigated Savonius turbines as an alternative for power generation in urban areas. Madina et al. [20] investigated the performance of vertical-axis wind turbines. Mauro et al. [21] conducted a numerical study to examine the effect of the duct blockage on the performance of the Savonius wind turbine's rotor. Nasef et al. [22] numerically investigated the performance of the Savonius rotor for different overlap ratios using different turbulence models. Al-Ghriybah et al. [23] improved the performance of Savonius turbines by placing the inner blades on conventional Savonius blades. Ramarajan et al. [24] conducted a study on the performance of the Savonius turbine with various interior turbine parameters. Tian et al. [25] conducted a study of the power efficiency of the Savonius turbine with different convex and concave blades.

In the present study, in order to increase the performance of Savonius wind turbines in dual turbine designs, a triangular plate was designed to prevent the flow from the blades rotating in the opposite direction and to direct it to the other blades that produces a positive torque. By examining the geometric parameters of this designed assembly, the turbine power performance was determined by establishing the parameters that provide an increase in the optimum performance.

## 2. Design and Methods

With the present study, the performance of the Savonius wind turbine in designs with dual turbines rotating in opposite directions to each other was examined. To improve the performance of the Savonius wind turbine in the dual turbine design, a triangular plate was placed in front of the turbines. The effects of the geometric dimensions of this triangular plate which was placed on the turbine on its performance were studied. With this triangular plate, it was ensured that the negative torque generated during the operation of Savonius wind turbines, especially due to their construction, was reduced and the flow was directed to the concave blade that produces a positive torque. Thus, the performance values of the Savonius wind turbine were increased. The methodology of the study for this purpose is shown in Figure 1. The accuracy of the numerical analysis was ensured before the performance improvement studies. A reference performance analysis of the conventional Savonius wind turbine was performed with a numerical analysis, the accuracy of which was proven by the experimental data. During the reference performance studies, an analysis of one of the Savonius wind turbines in the dual turbine design was also carried out. In the comparison analyses conducted throughout the study, one of the Savonius wind turbines in the dual turbine design was considered. Finally, the performance improvement studies were carried out. In those studies, the geometric parameters of the triangular plate in the case of a dual use of the Savonius wind turbines were discussed and examined, by comparison.

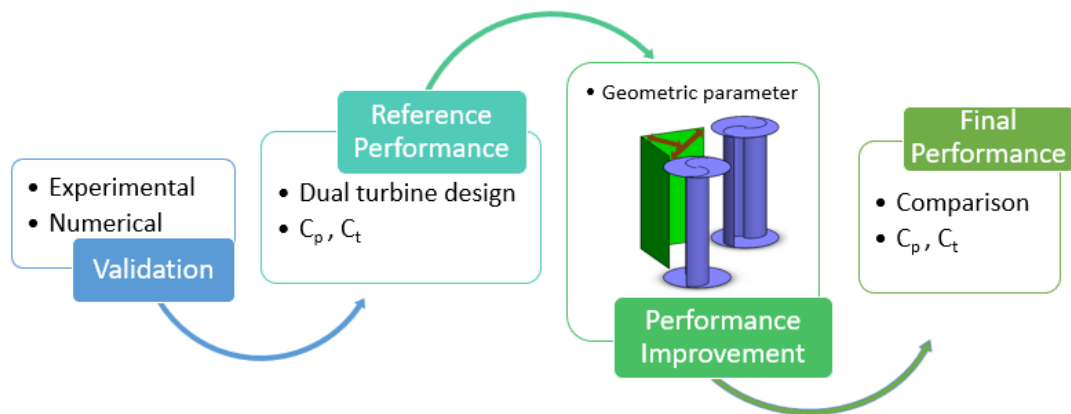


**Figure 1.** Study Methodology.

The performance analyses of the Savonius wind turbine under an 8.2 m/s wind speed were performed using the program ANSYS Fluent. In the performance studies carried out for this, a dynamic analysis was performed with transient simulations depending on time. The power and torque coefficients were determined to assess the turbine's performance. The turbine torque and power coefficients were calculated using the average torque values produced by the turbine. The dimensions of the numerical flow domain were determined by the diameter of the Savonius wind turbine. The overall dimensions of the numerical flow domain are shown in Figure 2. The cross-sectional dimensions of the numerical flow domain were taken as  $10D \times 10D$ , considering the blocking effect in particular. The total numerical flow domain length was taken as  $16D$ . In order to perform a dynamic analysis, a rotating flow domain was created, as shown in the figure. In order to ensure a data transmission between the rotating and stationary flow domains, an interface was created between the rotating flow domain and the stationary flow domain.

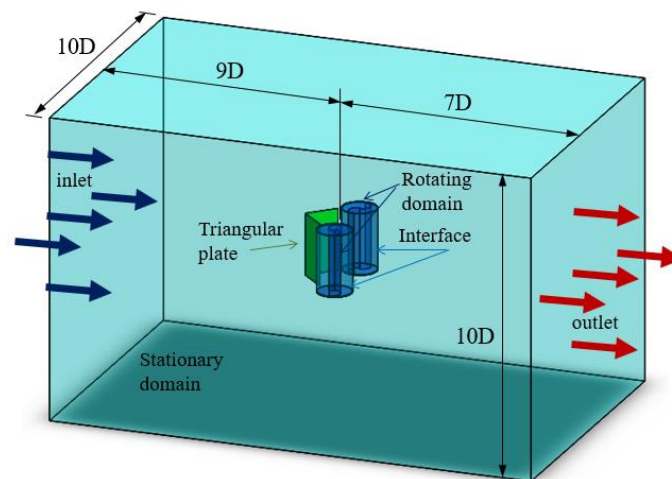


**Figure 2.** Numerical domains and boundaries.

Before the three-dimensional numerical analysis of the dual turbine designs of the Savonius wind turbine, three-dimensional numerical analyses were performed at different tip speed ratios on the single conventional Savonius wind turbine. The results of the numerical analysis were compared with the experimental results given by Deda Altan et al. [14] for a verification of the numerical solution method. All the conditions used in the comparison results, such as the conventional Savonius wind turbine and the flow domain, were taken according to this literature information. In this validation study, the unstructured grid for stationary and rotating domains was created around a conventional

Savonius turbine. The rotating and stationary flow domains were formed separately with triangular pyramid-type elements forming a mesh grid system. According to this literature, a standard k- $\epsilon$  turbulence model was used in the numerical solution method in the present study. This turbulence model was used the same in both the validation and performance studies. It is a Reynolds-averaged turbulence approach, most commonly known as the standard k-e model, which is a turbulence model with two equations. This model is a turbulence approach with a wide validity, and it gives highly suitable solutions for many industrial flow applications. In the numerical analysis, the minimum y+ dimensionless value was obtained at an average of 30. In addition to the iteration method, a secondary interpolation with a high reliability was used in the solutions. In the calculation of the pressure and velocity distributions, the semi-closed method (SIMPLE) solution algorithm was used for the pressure-dependent equations. For the performance comparisons, the same numerical mesh grid method was used throughout the study. In this way, the performance values obtained from different geometric parameters were compared and the best design conditions were determined.

The torque and power coefficients were calculated and compared with each other according to the data obtained from the numerical analysis. The turbine's performance was calculated using the torque coefficient ( $C_t$ ) given in Equation (1) and the power coefficient ( $C_p$ ) given in Equation (3). The tip speed ratio of the turbine was calculated with the tip speed ratio ( $\lambda$ ) given in Equation (6).

$$C_t = \frac{T}{T_{\text{available}}} \quad (1)$$

The  $T_{\text{available}}$  in the torque coefficient equation is calculated from Equation (2).

$$T_{\text{available}} = \frac{1}{4} \rho A V^2 D \quad (2)$$

$$C_p = \frac{P_{\text{turbine}}}{P_{\text{available}}} \quad (3)$$

The  $P_{\text{turbine}}$  and  $P_{\text{available}}$  in the power coefficient equation are calculated from Equations (4) and (5), respectively.

$$P_{\text{turbine}} = T \omega \quad (4)$$

$$P_{\text{available}} = \frac{1}{2} \rho A V^3 \quad (5)$$

$$\lambda = \frac{U}{V} = \frac{\omega D}{2V} \quad (6)$$

The  $\omega$  in the tip speed ratio equation is calculated from Equation (7)

$$\omega = \frac{2\pi n}{60} \quad (7)$$

In order to ensure the accuracy of the numerical analysis, the mesh independence study shown in Figure 3 was first carried out. The variation in the average torque coefficients according to the different mesh element numbers at a constant value of 0.335 of the turbine tip speed ratio is shown in the figure. As can be seen from the figure, it was determined that the average torque coefficient was obtained at almost the same values, especially in the 200,000 and subsequent cases of the number of mesh elements and did not change. In the numerical validation study, the number of mesh elements in the first case where the results did not change was considered.

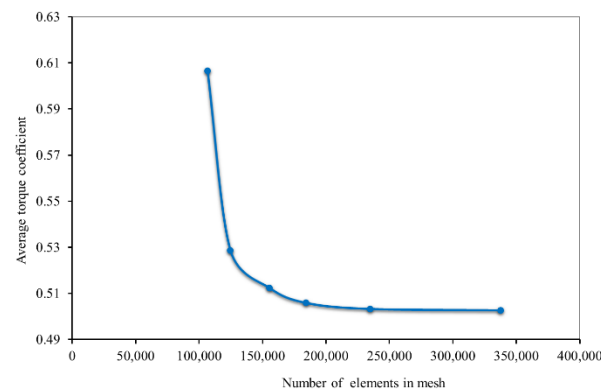


**Figure 3.** Mesh independence.

For the accuracy and stability of the numerical analysis, the time steps were determined when the results of the analysis obtained were almost the same. Thus, the time independence of the results of the analysis obtained was determined. The study of the time independence for the experimental torque coefficient [14] obtained at 0.335 of the tip speed ratio is shown in Figure 4. Here, one full revolution of the Savonius wind turbine was divided into 48-, 72-, and 144-time steps, respectively. The change in and averages of the torque coefficients of the turbine at a full revolution after the turbine enters the regime are shown in the figure. Considering the values of the average torque coefficients, it was determined that the average torque coefficient values obtained in the time steps after the 48-time steps were almost the same. Considering that the analysis time also increased with the increase in the time step, it was determined that the optimal time step was 48.

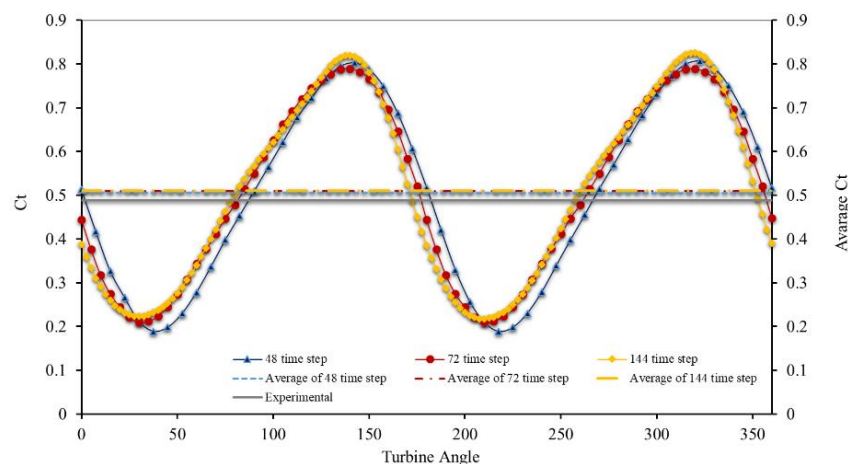


**Figure 4.** Time-step independence.

The comparison of the experimental torque coefficients given by Deda Altan et al. [14] and the variation of the average torque coefficient obtained by the numerical analysis is shown in Figure 5. In the regression analysis of the experimental and numerical data variations of the torque coefficients, the coefficient of the determination of the experimental data was obtained to be 0.9685 and the coefficient of the determination of the numerical model data was obtained to be 0.9535. The fact that the difference between the experimental and numerical model determination coefficients was obtained as low as 1.5% showed that the obtained variations generally overlapped with each other. As can be seen from the figure, the numerical results obtained were quite compatible with the experimental data. Thus, the validity of the numerical solution method was proven by comparing it with the experimental data. A numerical analysis, the accuracy of which was determined throughout the study, was used.

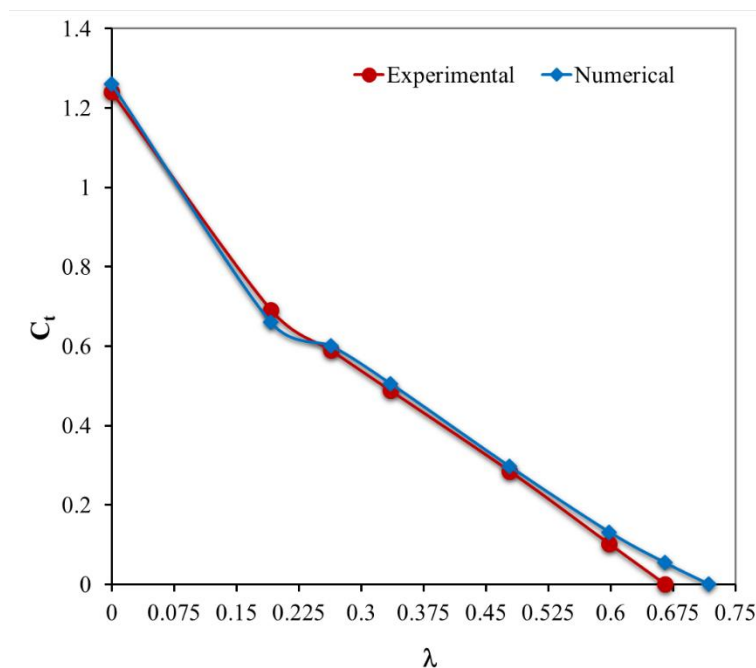


**Figure 5.** Validation of the numerical solution method with experimental data.

The geometric parameters of the triangular plate dual turbine design are shown in Figure 6. Each turbine in a dual turbine design is a Savonius wind turbine. The design parameters of the Savonius wind turbines used in the dual turbine design were also taken as the same. The design parameters of the Savonius wind turbine were kept constant throughout the study in order to examine the effects of the geometric dimensions of the triangular plate placed in front of the turbines and the geometric layout coordinates on the turbine's performance. The design parameters of the Savonius wind turbine were taken as the turbine diameter,  $D = 50$  cm, turbine height  $H = 100$  cm, the blade end plate diameter,  $D_0 = 1.1D$ , and the overlap ratio,  $e/d = 0.15$ . The geometric design parameters of the triangular plate dual Savonius wind turbines were taken as  $c$ : the distance between the turbine axes,  $a$ : the distance between the triangular plate and the turbine axes,  $b$ : the base width of the triangular plate,  $w$ : the tip width of the triangular plate, and  $\alpha$ : the triangular plate tip angle. The triangular plate height was taken as the same as the height of the Savonius wind turbine. The geometric parameters in the dual turbine design were designed in certain proportions according to the Savonius wind turbines used in the design. These design ratios were taken as the ratio of the distance between the turbine axes to the diameter of the Savonius wind turbine ( $c/D$ ), the ratio of the distance between the triangular plate and the turbine axes to the diameter of the Savonius wind turbine ( $a/D$ ), the ratio of the triangular plate base width to the diameter of the Savonius wind turbine ( $b/D$ ), and the ratio of the triangular plate tip width to the triangular plate base width ( $w/b$ ). By changing these design ratio values, the effects of these geometric parameters on the performance of the Savonius wind turbine were examined. During the study, the starting position of the Savonius wind turbines was taken so that the turbine blade was perpendicular to the wind flow direction, as can be seen from Figure 6. The blades of the turbines in the dual turbine design were opposite to each other in order to meet the wind flow.



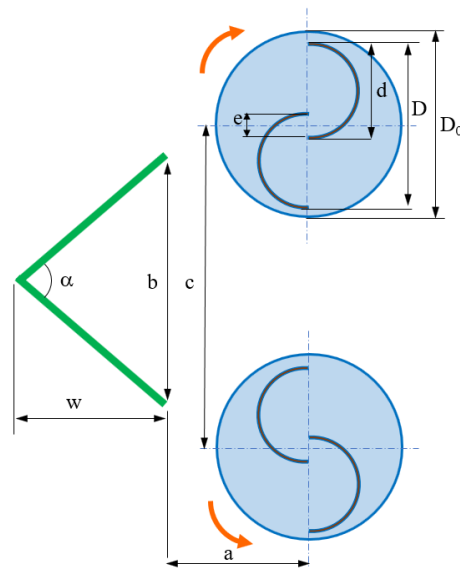


**Figure 6.** Geometric parameters of dual turbine design with triangular plate.

In Figure 7, the meshed cross-section of Savonius wind turbines in the dual turbine design, which was numerically analysed in this study, is shown. The grid mesh structure was created using the ANSYS-Meshing interface. Rotating and stationary flow domains were formed separately by tetrahedrons-type elements. An unstructured mesh system was used here. Throughout the study, numerical analysis verified by experimental data was used.

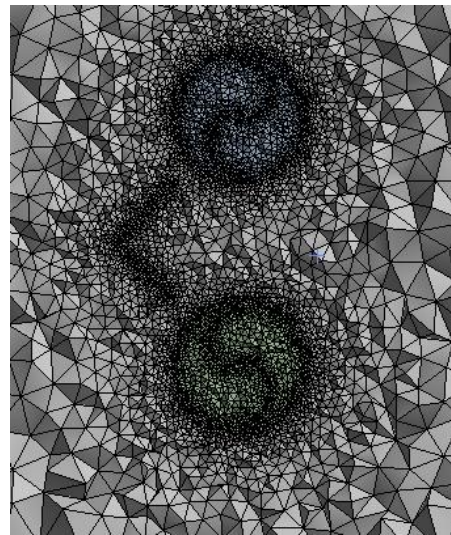


**Figure 7.** Mesh structure of dual turbine design.

### 3. Results and Discussion

In the present study, the effect of the triangular plate on the performance of the dual Savonius wind turbines that were reversed relative to each other was examined numerically. For this purpose, the variations in the torque and power coefficients of the turbines were determined. In order to increase the performance of the dual turbine designs, triangular plates were placed in front of the dual Savonius wind turbines to examine the increases in the turbine performance. In order to examine and compare these performance increases, the dual turbine design with the conventional Savonius wind turbine was discussed as a reference. In order to be able to examine and compare these performance increases, firstly,



the conventional Savonius wind turbine and the dual turbine design were discussed as a reference. The change in the power coefficient for a Savonius wind turbine in a dual turbine design with a conventional Savonius wind turbine, according to the turbine tip speed ratio, is shown in Figure 8. The power coefficient change was obtained here by numerical analysis from the average torque coefficients produced by the turbine. In the dual turbine design, the distance between the turbine axes was taken according to the fact that the  $c/D$  ratio was 2.2. As can be seen from the figure, it was found that the power coefficient changes obtained for both cases were almost similar to each other and were very close values. Therefore, it was determined that Savonius wind turbines in the dual turbine design were not affected by each other in the distance between these turbine axes. The maximum power coefficient for both the conventional Savonius wind turbine and the Savonius wind turbine in the dual turbine design was found with a turbine tip speed ratio of approximately 0.638. In order to examine the performance increase effects of the triangular plate used in the dual turbine design on the turbine, numerical analyses were performed throughout the study at a 0.638 turbine tip speed ratio, where the maximum power coefficient was obtained.

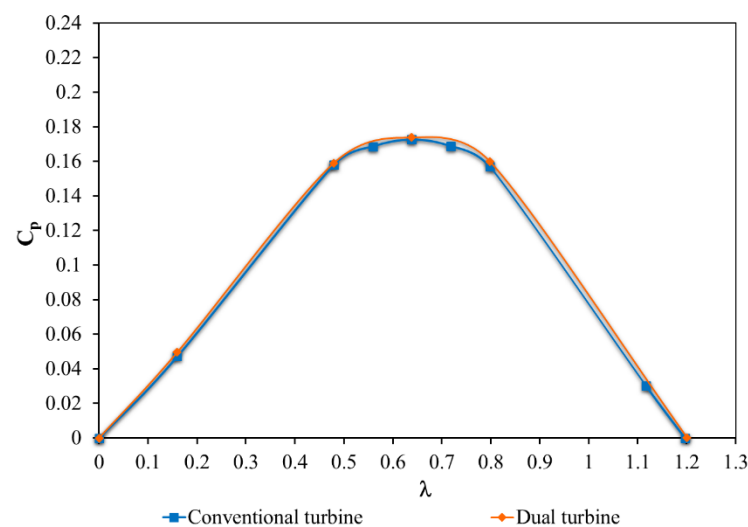


**Figure 8.** The power coefficients of the reference conventional and dual turbine.

The effect of the triangular plate tip width on the torque coefficient variation in a triangular plate dual turbine design is shown in Figure 9. The changes in the resulting torque coefficients were determined from a complete turbine rotation after the turbine entered the stable regime. In order to compare the results obtained, the value of the turbine tip speed ratio was taken as constant, i.e., 0.638. The other geometric parameters were also taken as constant to examine the effect of the triangular plate tip width on the torque coefficient. According to this, the distance between the turbine axes was taken according to 2.2 of the  $c/D$  ratio, the triangular plate base width was taken according to 2 of the  $b/D$  ratio, and the distance between the triangular plate and the turbine axes was taken according to 0.6 of the  $a/D$  ratio. With the values of 0.3, 0.5, and 0.9 of the ratios of the triangular plate end width to the triangular plate base width ( $w/b$ ), narrow ( $60^\circ$ ), perpendicular ( $90^\circ$ ), and wide ( $120^\circ$ ) triangular plate tip angles were formed, respectively. As can be seen from the figure, it was determined that the highest torque change was obtained when the  $w/b$  ratio of the triangle plate tip width was 0.5. Moreover, the lowest torque change was achieved if the  $w/b$  ratio of the triangular plate tip width was 0.3. When the obtained torque changes were examined, the best torque values were obtained compared to the other angles if the triangular plate tip angle was  $90^\circ$ , i.e., the  $w/b$  ratio was 0.5.

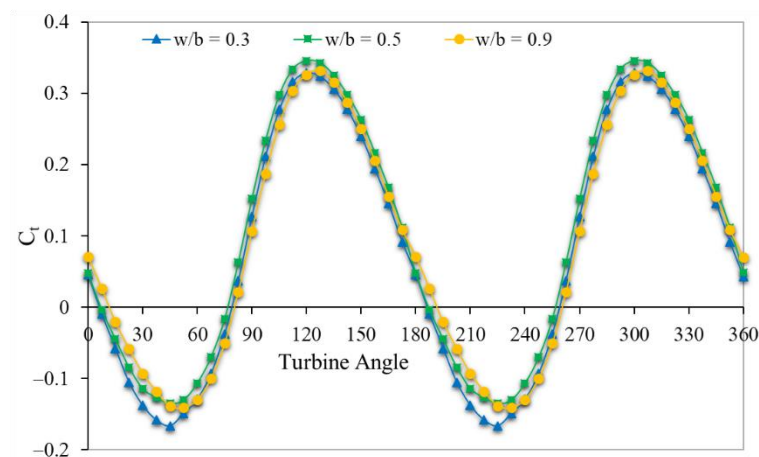


**Figure 9.** The effect of triangular plate end width.

The effect of the tip width of the triangular plate on the torque performance according to different  $w/b$  ratio values is shown by the velocity contours in Figure 10. Here, the distance between the turbine axes was taken as constant according to the fact that the  $c/D$  ratio was 2.2, the triangular plate base width was taken as constant according to the fact that the  $b/D$  ratio was 2, and the distance between the triangular plate and the turbine axes was taken as constant according to the fact that the  $a/D$  ratio was 0.6. It was observed that when the  $w/b$  ratio was 0.3 and 0.9, the flows directed to the concave blade of the turbine escaped more depending on the tip width of the triangular plate. In the case of the  $w/b$  ratio of 0.5, it was observed that the flow was directed towards the concave blade of the turbine, especially since the tip angle of the triangular plate was  $90^\circ$ .

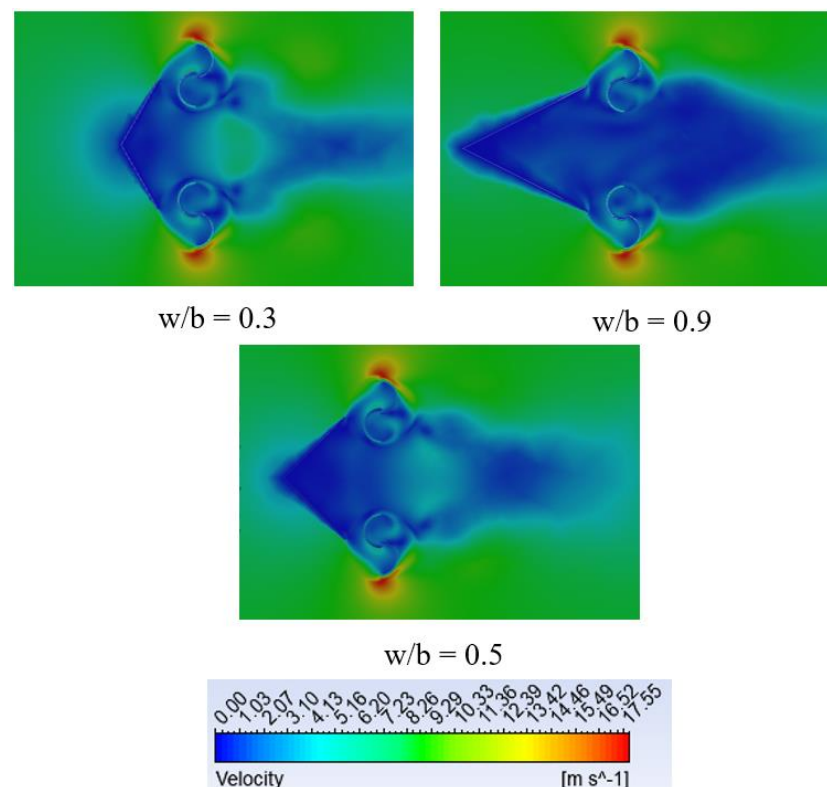


**Figure 10.** The effect of triangular plate end width with velocity contours.

The effects of different triangular base widths on the torque performance of the Savonius wind turbine in the triangular plate dual turbine design are shown in Figure 11. The variation in the torque coefficients in the conventional Savonius wind turbine was also demonstrated for a comparison. The variations in the resulting torque coefficients were determined from a complete turbine rotation after the turbine entered the regime. Numerical analyses were conducted according to the turbine tip speed ratio of 0.638. The distance between the turbine axes was taken as constant if the  $c/D$  ratio was 2.2, the distance between the triangular plate and the turbine axes was 0.6, and the  $w/b$  ratio of the triangular plate tip width was 0.5. As seen from the figure, if the  $b/D$  ratio was 1.4, the change in the torque coefficient obtained from the Savonius wind turbine in the triangular plate dual turbine design was almost the same as that of the conventional Savonius wind turbine. At values below this ratio, the change in the obtained torque coefficients was higher than the torque coefficient change obtained at this ratio. At ratios above this value, the change in the obtained torque coefficients was lower than the torque coefficient change obtained at this ratio. It was determined that negative values occurred in the torque changes at 1.4 and above the values of the  $b/D$  ratio. Since this negative formation adversely affects the average torque coefficient of the turbine, it causes the turbine performance value to decrease. It was determined that if the  $b/D$  ratio was two, the resulting torque coefficient change was at the lowest values. If the  $b/D$  ratio was one, it was determined that the resulting torque coefficient change was at the highest values.

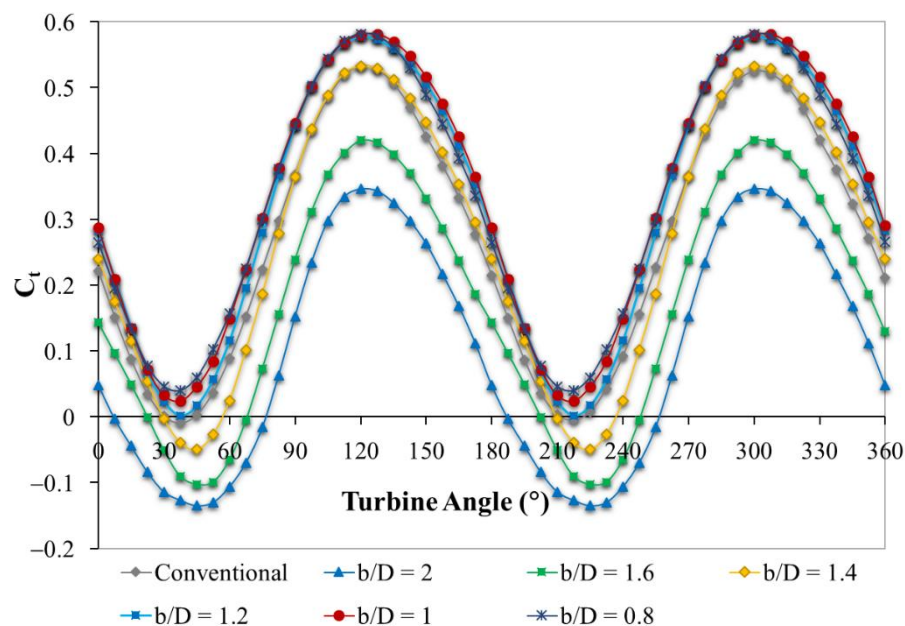


**Figure 11.** The effect of triangular plate base width.

The average of the torque coefficients obtained from a full rotation of the Savonius wind turbine at different  $b/D$  ratios under a fixed tip speed ratio of 0.638 is shown in Figure 12. In addition, the average torque performance of the conventional Savonius wind turbine is also shown in the figure to compare the torque performances. When the obtained data were compared with the conventional Savonius wind turbine, in the triangular plate dual turbine design, it was determined that the Savonius wind turbine had a higher average torque performance at values below 1.4 in the  $b/D$  ratio. At values above 1.4 of the  $b/D$  ratios, it was determined that it had a lower average torque performance than the conventional Savonius wind turbine. The average torque coefficient of the  $b/D$  ratio at a value of 1 was the maximum around 0.33. Thus, it was determined that the torque performance of the conventional Savonius wind turbine with its triangular plate dual turbine design increased from 0.27 to around 0.33.

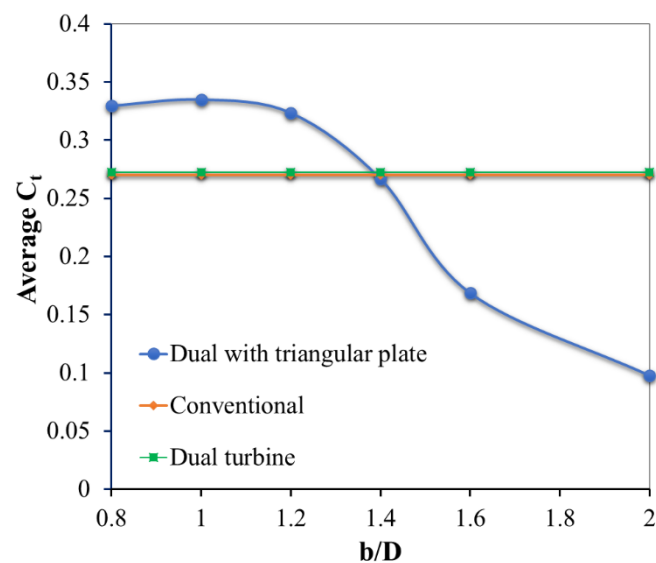


Figure 12. Comparison of torque coefficients.

The velocity contours according to the different  $b/D$  ratio values of the base width of the triangular plate are shown in Figure 13. Here, the  $c/D$  ratio was taken as 2.2, the  $a/D$  ratio was 0.6, and the  $w/b$  ratio was 0.5. It was observed that the flow did not enter the concave blade of the turbine at large values of the  $b/D$  ratio. When evaluated together with Figure 12, it was found that the best flow routing occurred when the  $b/D$  ratio was 1.

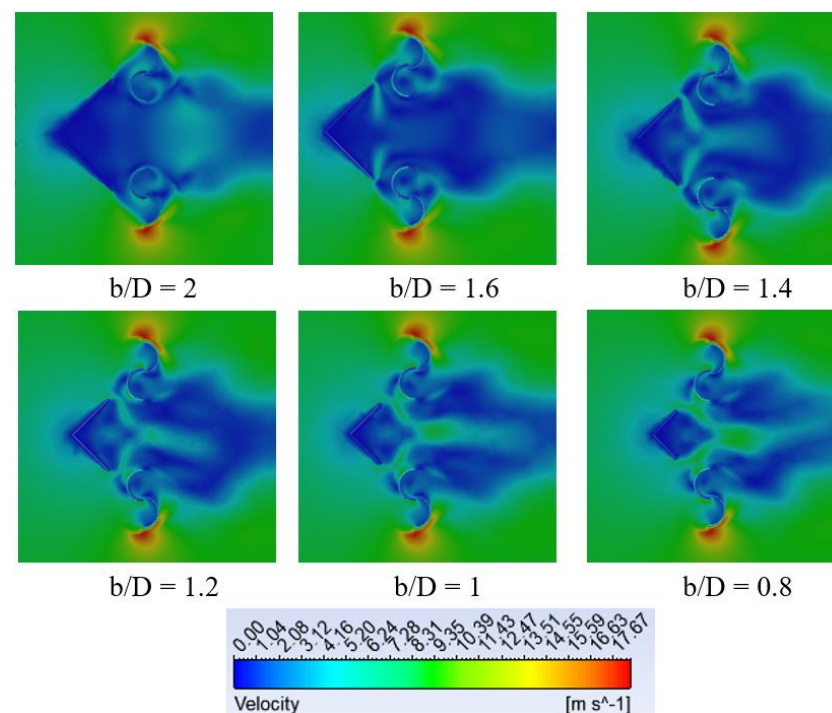
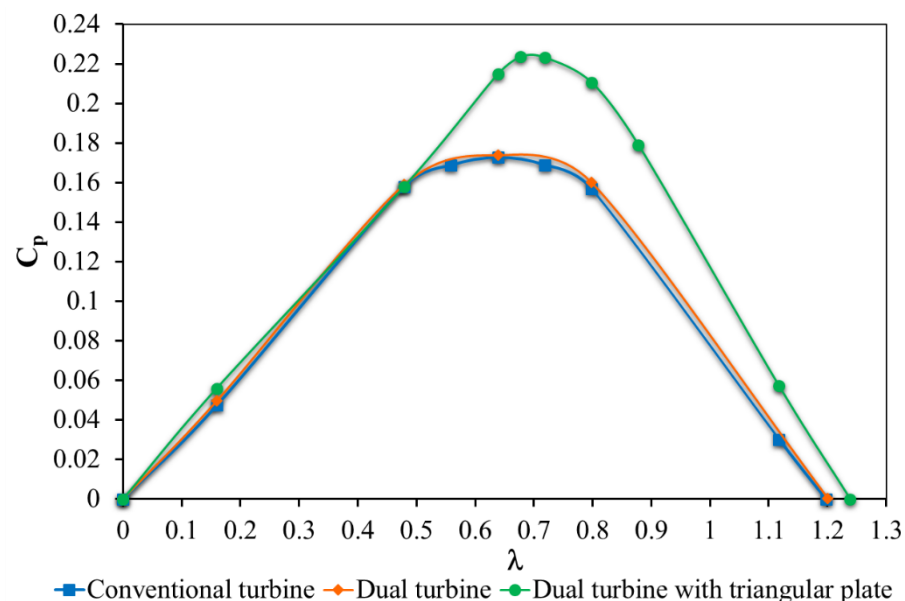


Figure 13. The effect of triangular plate base width with velocity contours.

In Figure 14, the variation in the power coefficient obtained in the case of a conventional, dual, and triangular plate dual use of the Savonius wind turbine according to the tip speed ratio is shown. In the dual turbine design, the  $c/D$  ratio was taken as 2.2. As seen from the figure, the power coefficient changes in the conventional Savonius wind turbine and the Savonius wind turbine in the dual turbine design were similar to each other, and the maximum power coefficient was around 0.17 with a turbine tip speed ratio of about

0.638. In the triangular plate dual turbine design, the  $a/D$  ratio was taken as 0.6, the  $b/D$  ratio was 1, and the  $w/b$  ratio was taken as 0.5. In the triangular plate dual design, the maximum power coefficient of the Savonius wind turbine was obtained around 0.22. This maximum power coefficient was found at a turbine tip speed ratio of about 0.676. The increase in the turbine tip speed ratio compared to that of the conventional Savonius wind turbine also showed that the rotational speed of the turbine increased. When all these results were examined, it was found that the power coefficient obtained by the Savonius wind turbine in the triangular plate dual design was around 30% higher compared to the power coefficient of the conventional Savonius wind turbine.



**Figure 14.** The effect of the triangular plate on the power coefficient.

The comparison of the percentage increase in the improved power coefficient obtained with this study with other studies in the literature is given in Table 1. It is possible to classify the literature studies on this subject as additional designs made outside of [26] and structural designs made inside of Savonius wind turbines [27,28]. Here, additional guide design studies made in front of or around the turbine without any modifications to the conventional Savonius wind turbines with two semi-circular blades were evaluated. The increase in the obtained power coefficient was determined according to the conventional Savonius wind turbine. This study was determined to be quite efficient compared to other additional designs, especially when evaluated according to the percent increase in the power coefficient.

**Table 1.** Comparison of power coefficient improvement with previous studies.

Source	Number of Blades	Additional Guide Design Name	$C_p$ Increase (%)
Irabu ve Roy et al. [12]	Two	Guide-box tunnel	22.66
Tartuferi et al. [15]	Two	Conveyor-deflector curtain system	20.00
Yuwono et al. [29]	Two	Circular cylinder	12.23
Tian et al. [30]	Two	Passive deflector	24.91
Present study	Two	Triangular plate	30.00

#### 4. Conclusions

In this study, the effect of a triangular plate placed in front of the turbine on the performance of dual Savonius wind turbines rotating in the opposite direction was investigated.

In this direction, the optimal design parameters were determined, and the results obtained were evaluated by comparing them. In this context:

1. First of all, the numerical analysis used in the study was confirmed by the experimental data.
2. For comparison studies, the reference performance of the conventional Savonius wind turbine was determined.
3. The optimum design parameters of the triangular plate were determined by examining the variations in the torque coefficients obtained from the Savonius wind turbine in the dual turbine design.
4. The power coefficient of the conventional Savonius wind turbine at the tip speed ratio of 0.638 was determined to be approximately 0.17.
5. The maximum power coefficient of the dual Savonius wind turbine with triangular plates was determined at approximately 0.22.
6. Thus, it was determined that the power coefficient value of 0.17 increased to approximately 0.22.
7. The optimum design parameters for the maximum power coefficient obtained from the triangular plate dual Savonius wind turbine were determined as a  $c/D$  ratio of 2.2, a  $a/D$  ratio of 0.6, a  $b/D$  ratio of 1, and a  $w/b$  ratio of 0.5.

As a result, it was determined that the power coefficient increased by around 30% thanks to the triangular plate placed in front of the turbines during the dual turbine use of Savonius wind turbines. Thus, it was determined that the triangular plate made a significant contribution to the performance of the Savonius wind turbine by reducing the negative torque from the convex blade rotating in the opposite direction against the wind, directing the flow to the concave blade, producing a positive torque. In addition to the increase in the performance, the triangular-plate dual Savonius wind turbine system needs an additional system with a wind sensor in order to be directed towards the wind. Considering that this additional system can meet the energy required from time to time, depending on the change in the wind direction, from the energy it will produce itself, it shows the applicability of the system.

**Author Contributions:** Methodology, B.D.A. and A.G.; software, B.D.A.; validation, B.D.A.; formal analysis, B.D.A.; investigation, B.D.A.; resources, B.D.A. and A.G.; data curation, B.D.A. and A.G.; writing—original draft preparation, B.D.A. and A.G.; writing—review and editing, B.D.A. and A.G. All authors have read and agreed to the published version of the manuscript.

**Funding:** This research received no external funding.

**Data Availability Statement:** The data presented in this study are available on request from the corresponding author.

**Conflicts of Interest:** The authors declared no potential conflicts of interest with respect to the research, authorship, and/or publication of this article.

## Nomenclature

$a$	distance between the triangular plate and the turbine axes (m)
$b$	base width of the triangular plate (m)
$c$	distance between the turbine axes (m)
$d$	blade diameter (m)
$e$	gap distance (m)
$k$	turbulent kinetic energy ( $\text{m}^2/\text{s}^2$ )
$n$	rotational speed (rpm)
$w$	tip width of the triangular plate (m)
$A$	turbine swept area ( $\text{m}^2$ )
CFD	computational fluid dynamics
$C_p$	power coefficient
$C_t$	torque coefficient



D	diameter of Savonius wind turbine (m)
$D_0$	blade end plate diameter (m)
H	turbine height (m)
SIMPLE	Semi-Implicit Methods for Pressure Linked Equations
T	torque (Nm)
U	turbine tip speed (m/s)
V	wind speed (m/s)
y+	dimensionless wall distance
$\alpha$	triangular plate tip angle
$\varepsilon$	turbulent kinetic energy dissipation rate
$\lambda$	tip-speed ratio
$\rho$	density (kg/m <sup>3</sup> )
$\omega$	angular velocity (rad/s)

## References

1. Hashem, I.; Mohamed, M.H. Aerodynamic performance enhancements of H rotor Darrieus wind turbine. *Energy* **2018**, *142*, 531–545. [\[CrossRef\]](#)
2. Sagimbayev, S.; Kylyshbek, Y.; Batay, S.; Zhao, Y.; Fok, S.; Lee, T.S. 3D multidisciplinary automated design optimization toolbox for wind turbine blades. *Processes* **2021**, *9*, 581. [\[CrossRef\]](#)
3. Hu, D.; Deng, L.; Zeng, L. Study on the aerodynamic performance of floating offshore wind turbine considering the tower shadow effect. *Processes* **2021**, *9*, 1047. [\[CrossRef\]](#)
4. Gao, Z.; Liu, X. An Overview on Fault Diagnosis, Prognosis and Resilient Control for Wind Turbine Systems. *Processes* **2021**, *9*, 300. [\[CrossRef\]](#)
5. Santhakumar, S.; Palanivel, I.; Venkatasubramanian, K. A study on the rotational behaviour of a Savonius Wind turbine in low rise highways during different monsoons. *Energy Sustain. Dev.* **2017**, *40*, 1–10. [\[CrossRef\]](#)
6. Abdelaziz, K.R.; Nawar, M.A.A.; Ramadan, A.; Attai, Y.A.; Mohamed, M.H. Performance improvement of a Savonius turbine by using auxiliary blades. *Energy* **2022**, *244*, 122575. [\[CrossRef\]](#)
7. Norouztabar, R.; Ajarostaghi, S.S.M.; Mousavi, S.S.; Nejat, P.; Koloor, S.S.R.; Eldessouki, M. On the performance of a modified triple stack blade Savonius wind turbine as a function of geometrical parameters. *Sustainability* **2022**, *14*, 9816. [\[CrossRef\]](#)
8. Lee, J.H.; Lee, Y.T.; Lim, H.C. Effect of twist angle on the performance of Savonius wind turbine. *Renew. Energy* **2016**, *89*, 231–244. [\[CrossRef\]](#)
9. Sharma, S.; Sharma, R.K. CFD investigation to quantify the effect of layered multiple miniature blades on the performance of Savonius rotor. *Energy Convers. Manag.* **2017**, *144*, 275–285. [\[CrossRef\]](#)
10. Al Absi, S.M.; Jabbar, A.H.; Mezan, S.O.; Al-Rawi, B.A.; Al Attabi, S.T. An experimental test of the performance enhancement of a Savonius turbine by modifying the inner surface of a blade. *Mater. Today Proc.* **2021**, *42*, 22332240. [\[CrossRef\]](#)
11. Manganhar, A.L.; Rajpar, A.H.; Luhur, M.R.; Samo, S.R.; Manganhar, M. Performance analysis of a Savonius vertical axis wind turbine integrated with wind accelerating and guiding rotor house. *Renew. Energy* **2019**, *136*, 512–520. [\[CrossRef\]](#)
12. Irabu, K.; Roy, J.N. Characteristics of wind power on Savonius rotor using a guide-box tunnel. *Exp. Therm. Fluid Sci.* **2007**, *32*, 580–586. [\[CrossRef\]](#)
13. Deda Altan, B.; Atilgan, M. The use of a curtain design to increase the performance level of a Savonius wind rotors. *Renew. Energy* **2010**, *35*, 821–829. [\[CrossRef\]](#)
14. Deda Altan, B.; Atilgan, M.; Ozdamar, A. An experimental study on improvement of a Savonius rotor performance with curtaining. *Exp. Therm. Fluid Sci.* **2008**, *32*, 1673–1678. [\[CrossRef\]](#)
15. Tartuferia, M.; D'Alessandro, V.; Montelpare, S.; Ricci, R. Enhancement of Savonius wind rotor aerodynamic performance: A computational study of new blade shapes and curtain systems. *Energy* **2015**, *79*, 371–384. [\[CrossRef\]](#)
16. Chang, T.L.; Tsai, S.F.; Chen, C.L. Optimal design of novel blade profile for Savonius wind turbines. *Energies* **2021**, *14*, 3484. [\[CrossRef\]](#)
17. Zhou, T.; Rempfer, D. Numerical study of detailed flow field and performance of Savonius wind turbines. *Renew. Energy* **2013**, *51*, 373–381. [\[CrossRef\]](#)
18. Goodarzi, M.; Salimi, S. Numerical assessment of the effect of different end-plates on the performance of a finite-height Savonius turbine. *Energy Sources Part A Recov. Util. Environ. Eff.* **2021**, *2021*, 324. [\[CrossRef\]](#)
19. Mereu, R.; Federici, D.; Ferrari, G.; Schito, P.; Inzoli, F. Parametric numerical study of Savonius wind turbine interaction in a linear array. *Renew. Energy* **2017**, *113*, 1320–1332. [\[CrossRef\]](#)
20. Madina, F.G.; Gutierrez, A.; Galione, P. Computational fluid dynamics study of Savonius rotors using Open FOAM. *Wind Eng.* **2021**, *45*, 630–647. [\[CrossRef\]](#)
21. Mauro, S.; Brusca, S.; Lanzafame, R.; Messina, M. CFD modelling of a ducted Savonius wind turbine for the evaluation of the blockage effects on rotor performance. *Renew. Energy* **2019**, *141*, 28–39. [\[CrossRef\]](#)
22. Nasef, M.H.; El-Askary, W.A.; Abdel-Hamid, A.A.; Gad, H.E. Evaluation of Savonius rotor performance: Static and dynamic studies. *J. Wind Eng. Ind. Aerodyn.* **2013**, *123*, 1–11. [\[CrossRef\]](#)



23. Al-Ghriybah, M.; Fadhli Zulkafli, M.; Hissein Didane, D.; Mohd, S. The effect of spacing between inner blades on the performance of the Savonius wind turbine. *Sustain. Energy Technol. Assess.* **2021**, *43*, 100988. [[CrossRef](#)]
24. Ramarajan, J.; Jayavel, S. Numerical study of the effect of geometry and operating parameters on the performance of Savonius vertical axis wind turbine. *Curr. Sci.* **2020**, *119*, 1927–1938. [[CrossRef](#)]
25. Tian, W.; Mao, Z.; Zhang, B.; Li, Y. Shape optimization of a Savonius wind rotor with different convex and concave sides. *Renew. Energy* **2018**, *117*, 287–299. [[CrossRef](#)]
26. Youssef, K.M.; El Kholy, A.M.; Hamed, A.M.; Mahmoud, N.A.; El Baz, A.M.; Mohamed, T.A. An innovative augmentation technique of Savonius wind turbine performance. *Wind Eng.* **2020**, *44*, 93–112. [[CrossRef](#)]
27. Chan, C.M.; Bai, H.L.; He, D.Q. Blade shape optimization of the Savonius wind turbine using a genetic algorithm. *Appl. Energy* **2018**, *213*, 148–157. [[CrossRef](#)]
28. Mu, Z.; Tong, G.; Xiao, Z.; Deng, Q.; Feng, F.; Li, Y.; Arne, G.V. Study on aerodynamic characteristics of a Savonius wind turbine with a modified blade. *Energies* **2022**, *15*, 6661. [[CrossRef](#)]
29. Yuwono, T.; Sakti, G.; Aulia, F.N.; Wijaya, A.A.C. Improving the performance of Savonius wind turbine by installation of a circular cylinder upstream of returning turbine blade. *Alex. Eng. J.* **2020**, *59*, 4923–4932. [[CrossRef](#)]
30. Tian, W.; Bian, J.; Yang, G.; Ni, X.; Mao, Z. Influence of a passive upstream deflector on the performance of the Savonius wind turbine. *Energy Rep.* **2022**, *8*, 7488–7499. [[CrossRef](#)]